KSME Journal, Vol. 8, No. 3, pp. 325~331, 1994

Tensile Creep in Ceramics Using Four-Point Bending Test

Dong-Joo Lee* and Igor Palley**

(Received Febury 5, 1994)

A new model of ceramic creep in four point bending is proposed to determine the tensile creep rate which is difficult to test. Based on the assumption that ceramics creep only in tension and there is no creep in compression, the tensile creep rate of six ceramics is calculated in a simple way. The six ceramic compositions SiC, Al_2O_3/SiC, Mullite, Al_2O_3/Si_3N_4, Sialon and TZ-6Y, were subjected to a constant load which corresponded to initial maximum stress level of 135 MPa in four point bending. All tests were performed at 1100℃ for about 180 min. which is a time showing a steady short-time transient creep. Certain levels of creep, in terms of measured displacement, were observed in all the tested materials. The experiment shows that the lowest level of creep among the tested materials is in SiC, the highest is in TZ-6Y. The creep rate is expressed in terms of measured displacement and the calculated tensile creep rate at the apparent steady state is given for all tested materials.

Key Words: Ceramic, Tensile Creep Behavior, Strain Rate, Four-Point Bending, Neutral Axis, Tensile Stress

1. Introduction

A knowledge of the creep behavior of ceramic materials is of importance in computing their lifetime at high temperature. For brittle ceramic materials, the power-law creep parameters are commonly deduced from load-point displacement data generated by the four point bend experiments under the assumption that tensile and compressive behaviors obey the same constitutive law. However, because of microcracking and cavitation that preferentially occur under tension, it is now well recognized(Rosenfield and Shetty, 1985 ; Rosenfield et al., 1985) that this premise may not always be valid. Also, bend data reflect a combination of tensile and compressive responses, so the indivi dual effects of creep deformation and damage evolution cannot be distinguished readily.

For reasons of simplicity and economy, however, ceramic tensile responses are evaluated by bend tests(Carroll et al., 1988 ; Fett et al., 1988 ; Lin and Becher, 1990). There are also rigorous efforts to estimate the uniaxial creep behavior(Rosenfield et al., 1986 ; Chuang, 1986). Hollenberg et al.(1971) estimated the stresses and strains in the four point flexural creep test by assuming a neutral axis in the midplane of the flexure specimen. This method was widely used to interpret load-point displacement versus time for variously fixed loads on separate specimens until recently(Ferber et al., 1990). Chuang(1986) presented the governing equations to derive the location of the neutral axis of a beam under bending which does not pass through the centroid of the cross section, and for the creep response in terms of both curvature rate and load-point displacement rate as functions of the applied moment and power-law creep parameters. Krause(1992), however, pointed out that curvature rates can not be measured with sufficient accuracy to determine the power-law parameters for tensile creep. Also, Chuang's analysis is awkward to execute and its accuracy is limited to the size of the incremented step in the curvature rate

*Deptartment of Mechanical Engineering Yeungnam University, Gyungsan, Gyungbuk 712-749
**Corporate Research and Technology, Allied-Signal Inc. Morristown, N. J. 07962

generated in his approximation.

The objectives of this study were to offer a simple analysis of tensile creep levels in terms of strain rates which would be observed in uniform tension using the data of the bending creep test. By introducing certain hypotheses on the creep and subsequent mathematical modeling of the situation, the tensile creep levels in terms of strain rates were obtained for the brittle ceramic materials using four point bending test. Also, the creep test is performed to compare the resistance to tensile creep of six ceramic compositions which are considered to be candidates for high temperature applications. The six ceramic compositions are SiC, Al_2O_3/SiC, Mullite, Al_2O_3/Si_3N_4, Sialon and TZ-6Y.

2. A Simplified Model of Tensile Creep during Four-Point Bending

As it is evident from the analysis of respective literature(Chuang and Weiderhorn, 1988; Dryden and Watt, 1981), most ceramic materials creep in tension much more easily than in compression. Presence of such creep micromechanisms as growth of pores or grain boundary sliding account for the difference. By assuming the absence of creep in compression, this is actually considering the limited case and in order to obtain a simple closed form solution, two major assumptions are made:

1. Material creeps only in tension and there is no creep in compression.
2. Stress is distributed across the extended part of the cross section as shown in Fig. 1.

Then, strain rate($\dot{e}_c$) dependence on the tensile stress(σ_t) according to existing experimental data can be approximated by a power-law in the steady state

$$\dot{e}_c = \alpha \sigma_t^{\beta} \tag{1}$$

where α and β are the material constants and always $\beta > 1$. The creep in a flexed beam is more intensive in the volumes of material which are closer to the tensile surface of the beam where the stresses are higher as shown in Fig. 1. The redistribution of stresses takes place during the initial period of creep, with a tendency to level the stress across the portion of the cross-section in tension. A rather complex computer simulation of the process of stress re-distribution(Fig. 2) is published in the literature(Dryden and Watt, 1981). It is clear that eventually this redistribution can be approximated by a simple one as shown in Fig. 1.

The model relationships are obtained on the basis of the following considerations: First, the central section of the beam is in pure bending, therefore, the cross sections which were plane before deformation remain plane after deformation including creep. These sections rotate against the neutral plane which position is defined by an ordinate y_0 from the outer compressed surface of

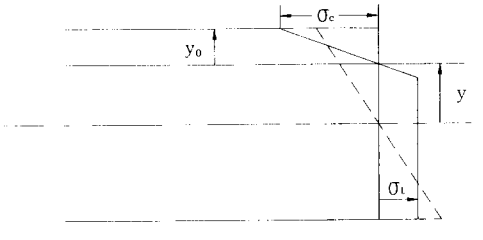

Fig. 1 Stress distribution due to bending

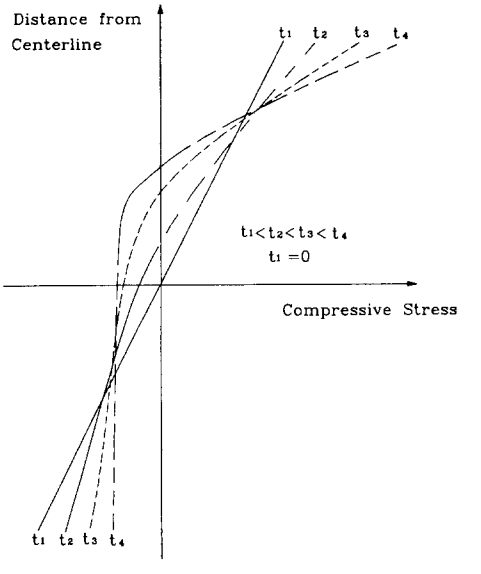

Fig. 2 Bending-stress redistribution at increasing times t_1, t_2, t_3 and t_4
(Dryden, J. R. and F., Watt, 1981)

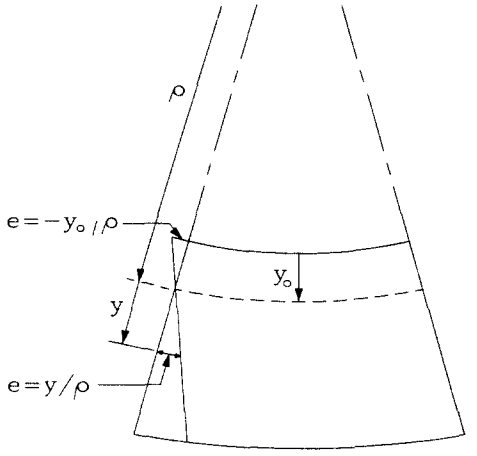

Fig. 3 Segment of a bent beam

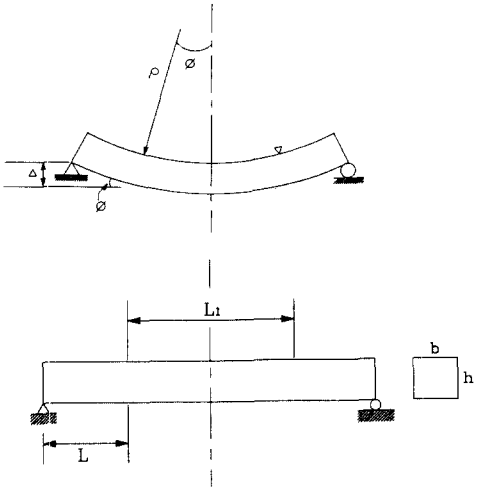

Fig. 4 Specimen geometry and deformed beam in bending

the beam. A beam has a rectangular cross section. The total beam height is h and its width is b(Fig. 4). The ordinate y_0 which before creep initiation is $y_0 = h/2$ becomes $y_0 < h/2$ and shifts monotonically toward the outer compression surface as the volumes in tension proceed creeping. A layer of the beam at distance y from the neutral layer(Fig. 3) experiences the total strain as

$$e = y/\rho \tag{2}$$

where ρ is the radius of the beam curvature. From the assumption on the absence of creep in compression and Eq. (2) follows an expression for the maximum stress in compression

$$\sigma_c = Ey_o/\rho \tag{3}$$

Two equations for the balance of external forces and internal stresses in cross section F are

$$\int_F \sigma dF = 0 \tag{4a}$$

$$\int_F y\sigma dF = M \tag{4b}$$

These can be used to establish a relationship among σ_t, the uniformly distributed tensile stress; y_o, the position of the neutral plane; M, the applied moment and ρ, the radius of curvature. One additional assumption, when writing out the integrals in Eqs. (4a) and (4b), simplifies the expressions while introducing a negligible imprecision for the case of a well developed creep. Namely, one assumes that the tensile stress, σ_t, is distributed uniformly across the whole area in tension and not as shown in Fig. 1. The difference in calculation of integrals(4a) and (4b) is small if a well developed state of creep is considered and the area where σ_t changes is small. Then, expression(4a) can be written out as

$$\sigma_t(h - y_o)b = \sigma_c y_o b/2 \tag{5}$$

Similarly, an expression(4b) as

$$\sigma_t(h - y_o)^2 b/2 + \sigma_c y_o^2 b/3 = M \tag{6}$$

By substituting Eq. (2) for Eqs. (5) and (6), one obtains

$$\sigma_t(h - y_o)/2 + Ey_o^2/2\rho \tag{7}$$

and

$$\sigma_t(h - y_o)^2/2 + Ey_o^3/3\rho = M/b \tag{8}$$

Expressing σ_t from Eq. (7) as

$$\sigma_t = \frac{Ey_o^2}{2(h - y_o)\rho} \tag{9}$$

and substituting for Eq. (8), one obtains a cubic algebraic equation with respect to an unknown y_o as follows

$$y_o^3 + 2h\ y_o = 12M\rho/bE \tag{10}$$

The radius of curvature, ρ, can be found as a function of the measured displacement, Δ(see Fig. 4) as

$$\rho = LL_1/2\Delta \tag{11}$$

where L and L_1 are the lengths of outer and inner

spans, respectively. If one assumed that the areas outside the inner span do not creep, Eqs. (10) and (11) allow one to find y_o as a function of M, Δ, E and the specimen geometry. Then, σ_t is found from Eq. (9). The corresponding strain rate can be found by using an expression for the maximum tensile strain,

$$e_{max}=(h-y_o)/\rho \tag{12}$$

Since e_{max} consists of two components as elastic and creep,

$$e_{max}=e^e_{max}+e^c_{max} \tag{13}$$

Since the elastic one is $e^e_{max}=\sigma_t/E$ and the creep component is e_c, one can write its as

$$\sigma_t/E+e_c=(h-y_o)/\rho \tag{14}$$

By differentiation of Eq. (14) with respect to time, one can find,

$$\dot{\sigma}_t/E+\dot{e}_c=-\dot{y}_o/\rho-(h-y_o)\dot{\rho}/\rho^2 \tag{15a}$$

from which

$$\dot{e}_c=-\dot{\sigma}_t/E-\dot{y}_o/\rho-(h-y_o)\dot{\rho}/\rho^2 \tag{15b}$$

For calculation of $\dot{e}_c$, the derivatives ρ, y_o and σ_t in Eq. (15b) can be expressed in terms of displacement rate, $\dot{\Delta}$. From Eq. (11)

$$\dot{\rho}=-LL_1\dot{\Delta}/2\Delta^2 \tag{16}$$

By solving Eqs. (10) and (11), a relationship between y_0 and Δ can be established. The calculated function $y_0=y_0(\Delta)$ is graphically presented in Fig. 5 in ln y_0 vs. ln Δ coordinates for the case of different values of modulus. The ln y_0 vs. ln Δ function turned out to be linear in the range of well developed creep, i. e. ln $y_0=k$ ln $\Delta+$ln c where slope $k=-0.93$ for $E=410$ GPa, $k=-0.92$ for $E=350$ GPa, $k=-0.90$ for $E=290$ GPa and $k=-0.78$ for $E=220$ GPa. Then, the derivative y_o can be analytically expressed through Δ as

$$\dot{y}_0=y_0k\dot{\Delta}/\Delta \tag{17}$$

From Eq. (9), one obtains

$$\dot{\sigma}_t=-\frac{y_o^2E}{2\Delta\rho(h-y_o)}\left[\frac{LL_1\dot{\Delta}}{2\Delta\rho}+\frac{(2h-y_0)k\dot{\Delta}}{(h-y_0)}\right] \tag{18}$$

By substituting Eqs. (16), (17) and (18) for Eq. (15). one obtains the following expression for $\dot{e}_c$ in terms of $\dot{\Delta}$, y_o and ρ:

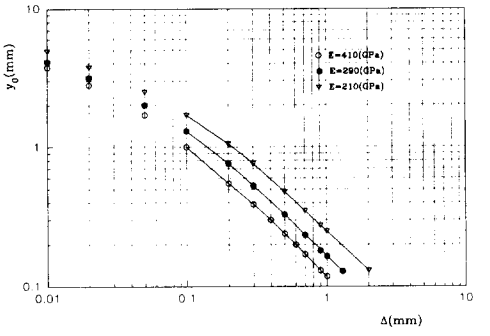

Fig. 5 Position of neutral axis as a function of modulus

$$\dot{e}_c=-\frac{\dot{\Delta}}{LL_1}\left[(h-y_o)-2ky_0-\frac{y_0^2}{(h-y_0)}\left\{1+\frac{(2h-y_0)k}{(h-y_0)}\right\}\right] \tag{19}$$

3. Experimental Procedures

Bars of 3 mm×4 mm were tested using four point bending with 20 mm inner(L_1) and 40 mm outer spans. The SiC fixture was used in these studies. The modulus of materials was determined with the strain gage in the tension side under four point loading. The 2100 multichannel system and the M-bond 200 kit from Micro-measurement Group Inc. was used to measure the strain and mount the strain gages respectively. The measured modulus of six ceramics is 410 GPa for SiC, 350 GPa for Al_2O_3/SiC, 290 GPa for Mullite, 280 GPa for Al_2O_3/Si_3N_4, 250 GPa for Sialon and 210 GPa for TZ-6Y.

The constant load was chosen to correspond the initial maximum values of constant stress equal 135 MPa. The constant load was applied and controlled with a precision of ±45 gram in the "load control" mode of Instron 1361 electromechanical tester. All tests were performed at 1100℃ for about 180 min. which is not enough time to get a secondary creep range but a steady short-time transient creep.

During the creep test, the actuator displacement, Δ, corresponding to the mutual displacement of external and supports(see Fig. 4) was measured and recorded as a function of time. A

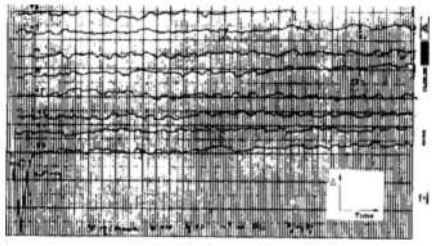

Fig. 6 A typicalF expeimental record of creep beha vior

typical $\Delta=\Delta(t)$ experimental record is shown in Fig. 6. An apparent steady creep rate, $\dot{\Delta}$, was calculated from such records in the short-time primary creep range.

4. Results and Discussion

In order to obtain the tensile creep rates for the tested materials using these experimental data, the model, described in the previous section, was applied. It is clear from the assumption on stress distribution(see Fig. 1) that the model should be only applied when the creep deformation reach an advanced stage. The calculations for the tested ceramics were typically performed starting from displacement $\Delta=0.10$ mm and ending at displacement $\Delta=0.8$ mm. The obtained plots of calculated tensile strain rates of all tested ceramics are shown in Fig. 7. According to the model, one can see that the tensile creep rates have not yet stabilized during the testing time. However, there is clear tendency to reach asymptotic values. The asymptotic estimates of creep strain rates for the tested materials are given in Table 1. Among the six ceramic compositions : SiC, Al_2O_3/SiC, Mullite, Al_2O_3/Si_3N_4, Sialon and TZ-6Y, the lowest level of creep among the tested materials is in SiC, the highest is in TZ-6Y.

If one assumes that the midplane of the specimen is the neutral axis of strain, then one can calculate the tensile strain, ϵ_{st}, from the simple elastic beam equation for small deflection as derived by Hollenberg et al.(1971).

$$\epsilon_{st}=3h\Delta/L(2L+3L_1) \tag{20}$$

Then, the tensile creep rate, $\dot{\epsilon}_{st}$, can be calculated as

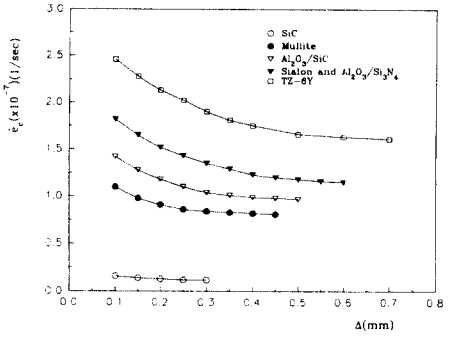

Fig. 7 The calulated tensile creep rate as a function of displacement

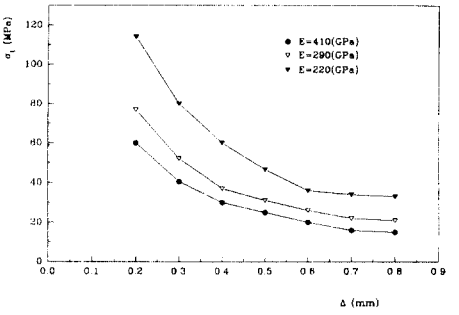

Fig. 8 The calulated tensile stress as a function of displacement and modulus

$$\dot{\epsilon}_{st}=3h\dot{\Delta}/\dot{L}(2L+3L_1) \tag{21}$$

The calculated $\dot{\epsilon}_{st}$ was also given in Table 1. Values of $\dot{\epsilon}_c$ and $\dot{\epsilon}_{st}$ have a same trend but quite different in magnitude. This difference is predicted due to the consideration of the midplane of the specimen as a neutral axis of strain. This assumption is not valid unless compressive and tensile creep are symmetrical in the materials.

The tensile stress level corresponding to these values is evidently not 135 MPa which was the initial maximum stress value. But an asymptotic value of 35 MPa for $E=220$ GPa, 23 MPa for $E=300$ GPa and 16 MPa for $E=410$ GPa is obtained from Fig. 8. This figure shows σ_t as a function of Δ and modulus of materials. As can be seen from the value, σ_t initially drops sharply from 135 MPa to 35~16 MPa, but does not significantly change for $\Delta>0.7$ mm as remaining in the range of 35~16 MPa. Again, this analysis assumed that the creep deformation reached an

advanced stage. Therefore, the tensile stress level under 0.3 mm of the displacement was not reliable. Also, this stress drop by the effect of the creep-induced stress relaxation is a little more severe than the values obtained by Ferber et al. (1990) that used the elastic analysis without changing the position of a neutral axis. As another approach of the simple elastic beam theory, but considering the change of neutral axis, the tensile stress for small deflection can be also calculated. Since the equilibrium of the forces acting on the cross section can be expressed by strain(ϵ) as $\epsilon = y/\rho$ and $dF = bdy$, then, $\int f(\epsilon) d\ \epsilon = 0$ from Eq. (4a) and $\int f(\epsilon)\epsilon\ d\epsilon = M(\epsilon/y)^2/b$ from Eq. (4b). By differentiating with respect to the curvature using Leibnitz' rule, one can obtain the outer tensile stress

$$\sigma_t = \frac{\dot{M}(\epsilon_t + \epsilon_c) + 2M(\dot{\epsilon}_t + \dot{\epsilon}_c)}{bh^2 \dot{\epsilon}_t} \tag{22}$$

For a small deflection of the beam under a static bending test, the change of moment is assumed to be zero. Since $\epsilon_t = (h - y_0)/\rho$ and $\epsilon_c = y_0/\rho$, one, then, obtains the corresponding tensile stress level from Eqs. (16) and (17) as

$$\sigma_t = \frac{FL}{Bh[(h - y_0) - y_0 k]} \tag{23}$$

By putting the $y_o = 1.5\Delta^{-k}$ from Fig. 5 for each different values of k($k = -0.44$ for $E = 220$ GPa and $k = -0.5$ for $E = 410$ GPa within the range of $\Delta < 0.1$ mm), the corresponding tensile stress level is calculated as shown in Fig. 9 as a function of

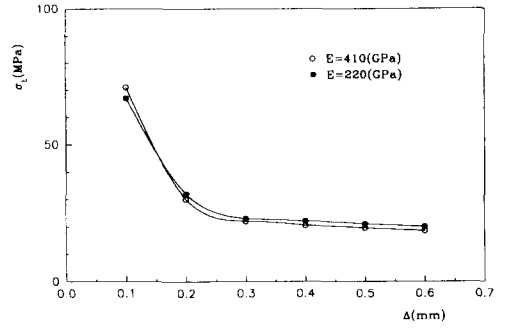

Fig. 9 The calulated tensile stress as a function of displacement and modulus

Table 1 The measured displacement rate($\dot{\Delta}$) and calculated creep rate($\dot{\epsilon}_c$ and $\dot{\epsilon}_{st}$) for five ceramics.

	$\dot{\Delta}$(mm/sec)	$\dot{\epsilon}_c$(1/sec)	$\dot{\epsilon}_{st}$(1/sec)
SiC	0.76×10^{-6}	0.14×10^{-7}	0.86×10^{-8}
Al_2O_3/SiC	6.04×10^{-6}	1.02×10^{-7}	6.79×10^{-8}
Mullite	4.83×10^{-6}	0.82×10^{-7}	5.43×10^{-8}
Al_2O_3/Si_3N_4	6.61×10^{-6}	1.16×10^{-7}	7.44×10^{-8}
Sialon	7.03×10^{-6}	1.15×10^{-7}	7.91×10^{-8}
TZ-6Y	9.92×10^{-6}	1.58×10^{-7}	11.2×10^{-8}

modulus. There seems to be a good correlation compared with Fig. 8 for high modulus materials but quite different for low modulus materials. As can be seen from the value, σ_t initially drops sharply from 135 MPa to 19 MPa without a significant change for $\Delta > 0.8$ mm. Since this analysis considers the position change of the neutral axis and doesn't have to be an advanced creep stage, k values are used for displacement less than 0.1 mm. However, there are no big differences depending on k values. But, the difference compared with Fig. 8 is no significant distinction between high and low modulus materials since Eq. (23) is not a function of modulus. Again, this stress drop by the effect of the creep-induced stress relaxation is more severe than the values obtained by Ferber et al.(1990) that used the elastic analysis without changing the position of a neutral axis. The direct comparision among flexural, compressive and tensile creeps of ceramic materials and the effects of assumption that there is no creep in compression will be published later.

5. Conclusions

A novel method of analysis is developed for evaluating the power-law parameters for tensile creep of structural ceramics at elevated temperature with four point bending creep data. Displacement rate, invariant with time in the apparent steady state creep, is measured on flexure specimens of the tested materials. The analysis takes into acount that a material behaves differently in

tensile and compression creep. Under the assumption that the tested ceramic materials do not creep in compression, those for tensile creep are calculated from displacement rate in the flexural creep tests in a simple way. The six ceramic compositions : SiC, Al_2O_3/SiC, Mullite, Sialon, Al_2O_3/Si_3N_4 and TZ-6Y, were subjected to a constant load which corresponds initial maximum stress level of 135 MPa in four point bending at 1100℃ for about 180 min and the rate of displacements were observed. The experiment shows that the lowest level of creep among the tested materials is in SiC, the highest is in TZ-6Y. The creep rate($\dot{\Delta}$) expressed in terms of measured displacement and the calculated tensile creep rate($\dot{e}_c$ and $\dot{\epsilon}_{st}$) at the apparent steady state are given in Table 1.

References

Carroll, D. F., Chuang, T. J. and Wiederhorn, S. M., 1988, "A Comparision of Creep Rupture Behavior in Tension and Bending," Ceram. Eng. Sci. Proc., Vol. 9, No. 8～9, pp. 635～642.

Chuang, T. J., 1986, "Estimation of Power-law Creep Parameters from Bend Test Data," J. Mater. Sci., Vol. 21, pp. 165～175.

Chuang, T. J. and Weiderhorn, S., 1988, "Damage-Enhanced Creep in a Siliconized Silicon Carbide : Mechanics of Deformation," of Amer. J. Ceram. Soc., Vol. 71, No. 7, pp. 595～601.

Dryden, J. R. and Watt, F., 1981, "Re-Distribution of Stresses During Creep-Bending of Grain Boundary Sliding Materials.," Surfaces and Interfaces in Ceramic and Ceramic-Metal Systems, Material Science Research, Vol. 19.

Ferber, M. K., Jenkins, M. G. and Tennery, V. J., 1990, "Comparision of Tension, Compression and Flexure Creep for Alumina and Silicon Nitride Ceramics," Ceram. Eng. Sci. Proc., 11 Vol. 11, No. 7～8, pp. 1028～1045.

Fett, T., Keller, K. and Munz, D., 1988, "An Analysis of the Creep of Hot Pressed Silicon Nitride in Bending," J., Mater. Sci., Vol. 23, pp. 467～474.

Hollenberg, G. W., Terwilliger, G. R. and Gordon, R. S., 1971, "Calculation of Stresses and Strains in Four-Point Bending Creep Tests," Amer. J. Ceram. Soc., Vol. 54, pp. 196～199.

Krause, R. F., Jr., 1992, "Observed and Theoretical Creep Rate for an Alumina Ceramic and a Silicon Nitride Ceramic in Flexure," J. Amer. Ceram. Soc., Vol. 75, No. 5, pp. 1307～1310.

Lin, H. T. and Becher, P. F., 1990, "Creep Behavior of a SiC-Whisker-Reinforced Alumina," J. of Amer. Ceram. Soc. Vol. 73, pp. 1378～1381.

Rosenfield, A. R. and Shetty, D. K., 1985, "Estimating Damage Laws from Bend-Test Data," J. of Mat. Sci., Vol. 20 No. 3, pp. 935～940.

Rosenfield, A. R., Shetty, D. K. and Duckworth, W. H., 1985, "Damage Analysis of Creep in Bending," J. of Amer. Ceram. Soc., Vol. 68, No. 9, pp. 483～485.

Rosenfield, A. R., Shetty, D. K. and Duckwort, W. H., 1986," Estimating Tensile Creep Data from Flexure Data," J. Amer. Ceram. Soc., Vol. 69, No. 5, pp. C108～C109.